Cell Reports, Volume *30*

Supplemental Information

TIFAB Regulates USP15-Mediated p53 Signaling during Stressed and Malignant Hematopoiesis

Madeline Niederkorn, Kathleen Hueneman, Kwangmin Choi, Melinda E. Varney, Laurel Romano, Mario A. Pujato, Kenneth D. Greis, Jun-ichiro Inoue, Ruhikanta Meetei, and Daniel T. Starczynowski

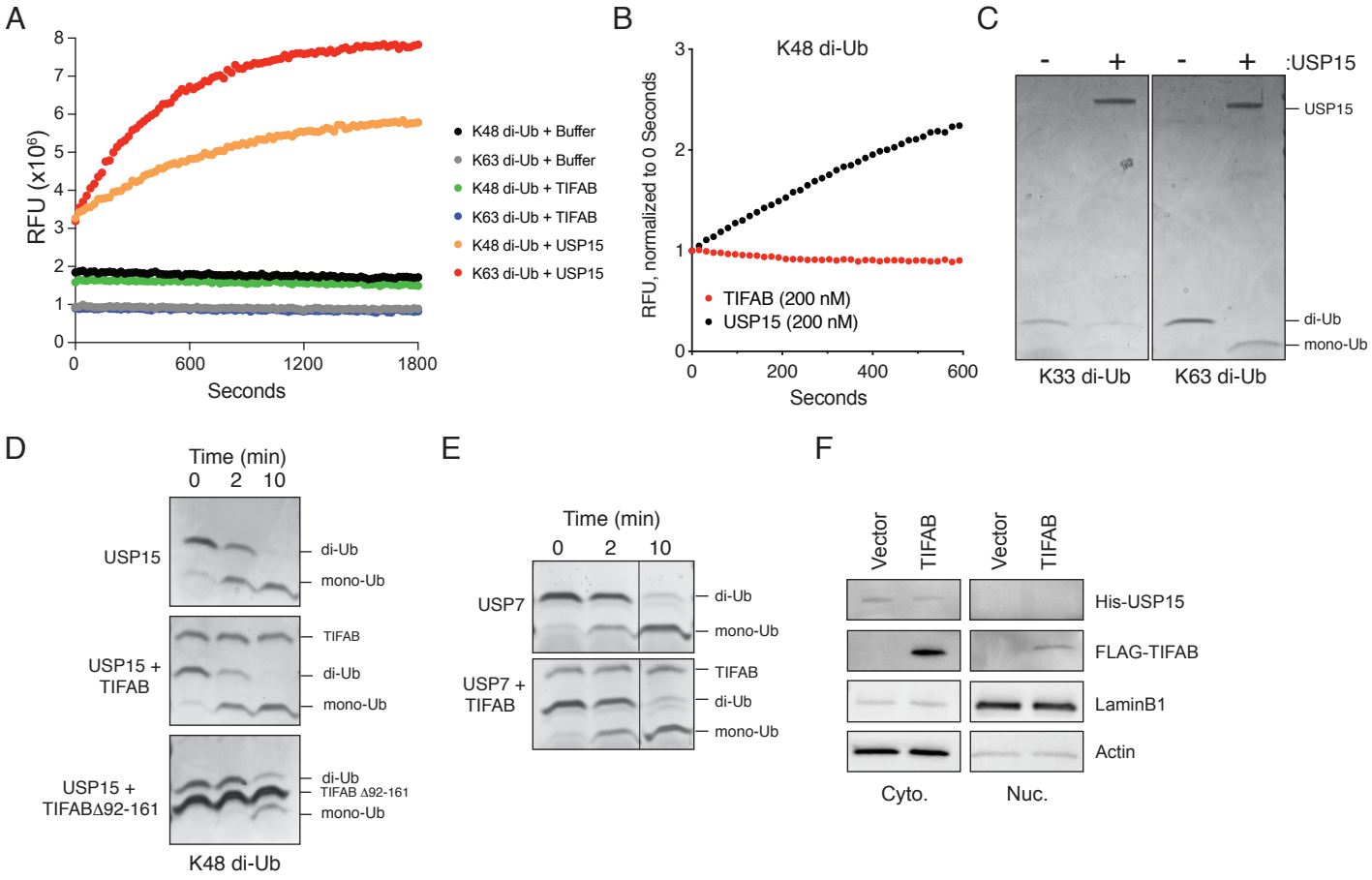

Figure S1. TIFAB lacks intrinsic catalytic activity and its effects in deubiquitination assays are specific to USP15 (related to Figure 2). (**A**) Relative fluorescence units (RFU) measured over time for IQF K48 and K63 linked di-ubiquitin (di-Ub) alone, with the addition of TIFAB eluate isolated from HL60-TIFAB lysate, or USP15. As a control, di-Ub alone or with TIFAB were evaluated. (**B**) Relative fluorescence generated by 200 nM of recombinant TIFAB (red) or 200 nM of recombinant USP15 (black) incubated with 200 nM IQF-K48 di-Ub substrates. (**C**) Coomassie-stained gel of di-ubiquitin hydrolysis reactions for 30 min in the absence or presence of USP15 enzyme. K33 di-Ub (left) and K63 di-Ub (right) were used as the substrate. (**D**) Coomassie-stained gel of di-Ub hydrolysis reactions at the indicated times with USP15 alone, USP15 with full-length recombinant TIFAB, and USP15 with a C-terminal deletion mutant of TIFAB. (**E**) Coomassie-stained gel of di-Ub hydrolysis reactions at the indicated times with USP7 alone, and USP7 with full-length recombinant TIFAB. (**F**) Immunoblotting of His-USP15 and FLAG-TIFAB in cytoplasmic and nuclear fractions of transfected HEK293 cells.

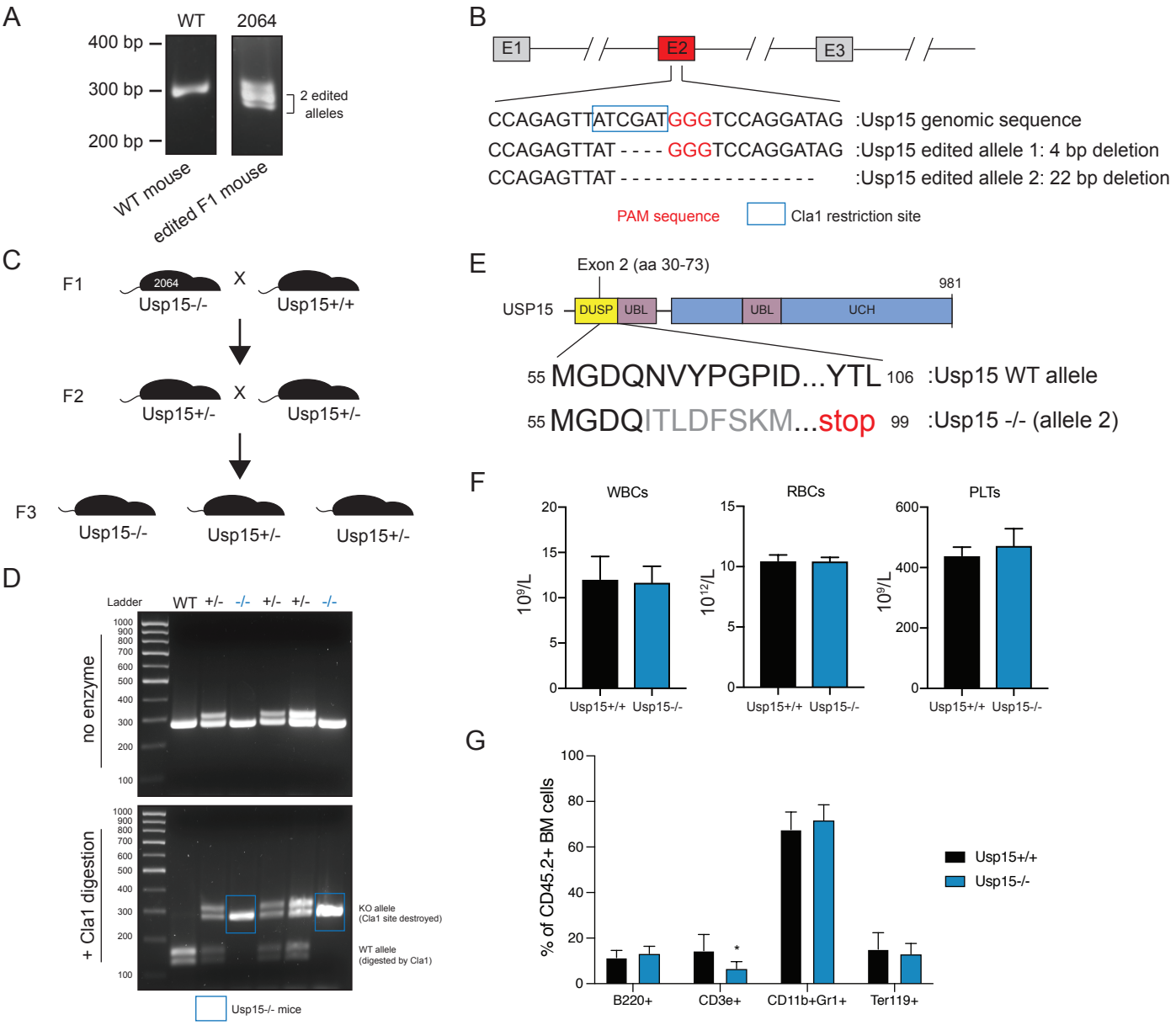

Figure S2. Generation of USP15 knockout mice (related to Figure 3). (A) DNA gel image of PCR amplification of the Usp15 locus in a WT control mouse and in an F1 mouse that was microinjected with a Usp15-targeted CRISPR-CAS9-guideRNA complex. Microinjection of mouse 2064 generated two modified alleles. (**B**) Schematic of Usp15 exon structure and gene targeting strategy. Guide RNAs were targeted to exon 2 of the Usp15 locus. Genomic sequence of Exon 2 for WT Usp15 and the two edited allele in F1 mouse 2064 is shown below. The PAM sequence directing the guide RNA activity is shown in red. Dashes represent identified 4 base-pair and 22 base-pair deletions in each respective allele. A Cla1 restriction enzyme site is present in the WT genetic sequence (blue box), but is destroyed in each edited allele. (**C**) Schematic of Usp15 knockout breeding strategy. The F1 mouse (2064) was crossed to a WT C57/Bl6 mouse to generate F2 heterozygous mice containing only one modified allele. Heterozygous mice were sequenced for Usp15 and mice with the identical modified allele were crossed to each other to generate homozygous edited mice (Usp15-/-). (**D**) Genotyping gel images of PCR amplification of Usp15 exon 2 for a litter from an F2 cross. To distinguish between WT and Usp15-/- mice, Cla1 digestion was performed. Genomic DNA from WT mice will result in digestion with Cla1 (2 bands below 200 bp). Genomic DNA from Usp15-/- mice is resistant to digestion with Cla1 resulting in 300 bp amplicon. (**E**) Schematic of full-length Usp15 protein, indicating the location of exon 2 and the predicted amino acid sequence of Usp15-/- mice (edited at allele 2), which will generate an N-terminal truncated protein. (**F**) Complete blood counts at 6 weeks post-transplant of lethally irradiated mice reconstituted with BM from Usp15+/+ and Usp15-/- mice.(**G**) Flow cytometry analysis of the indicated BM populations of lethally irradiated mice reconstituted with BM from Usp15+/+ and Usp15-/- mice (n = 15 per group). Error bars represent S.E.M. *, $P < 0.05$.

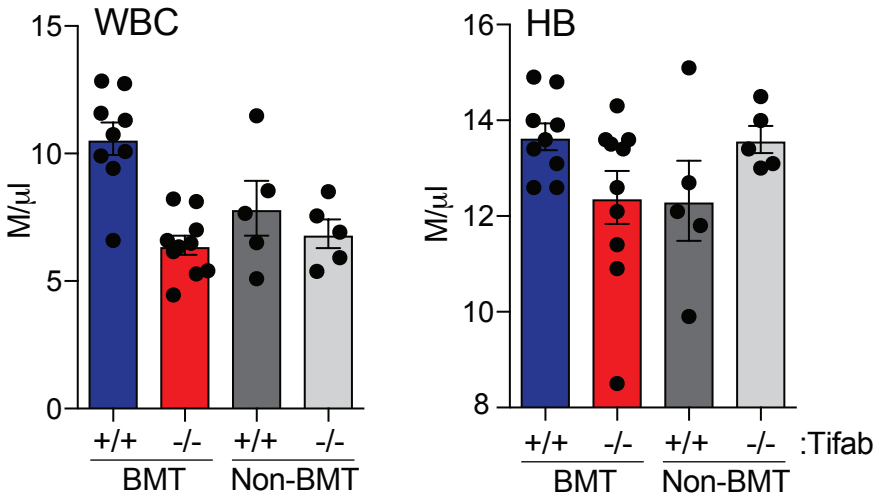

Figure S3. Transplantation of Tifab-deficient BM results in ineffective hematopoiesis (related to Figure 4). Blood counts were performed at ~6 months post-BM transplantation of Tifab+/+ or Tifab-/- BM cells into lethally-irradiated recipient mice. For non-transplanted mice, blood counts were performed at ~6 months of age. WBC, white blood cells; HB, hemoglobin.

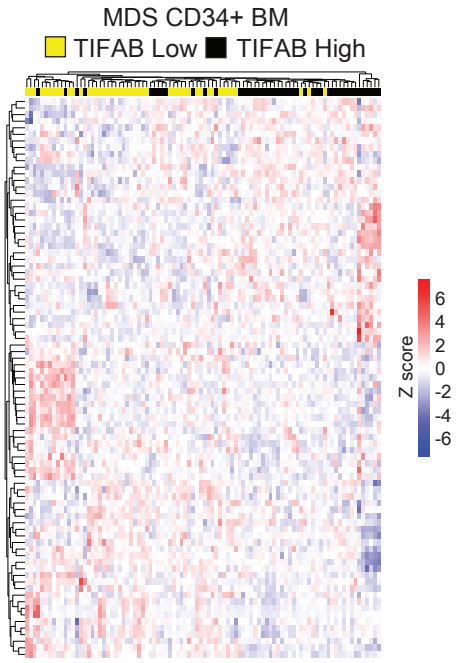

Figure S4. Differential gene expression in MDS CD34+ cells stratified based on TIFAB expression (related to Figure 4). Unsupervised hierarchical clustering and heat map showing expression differenes of p53 target genes in MDS CD34+ BM cells (n = 183) stratified based on TIFAB high (top quartile) and TIFAB low (bottom quartile) expression (Pellagatti et al., Leukemia, 2010).

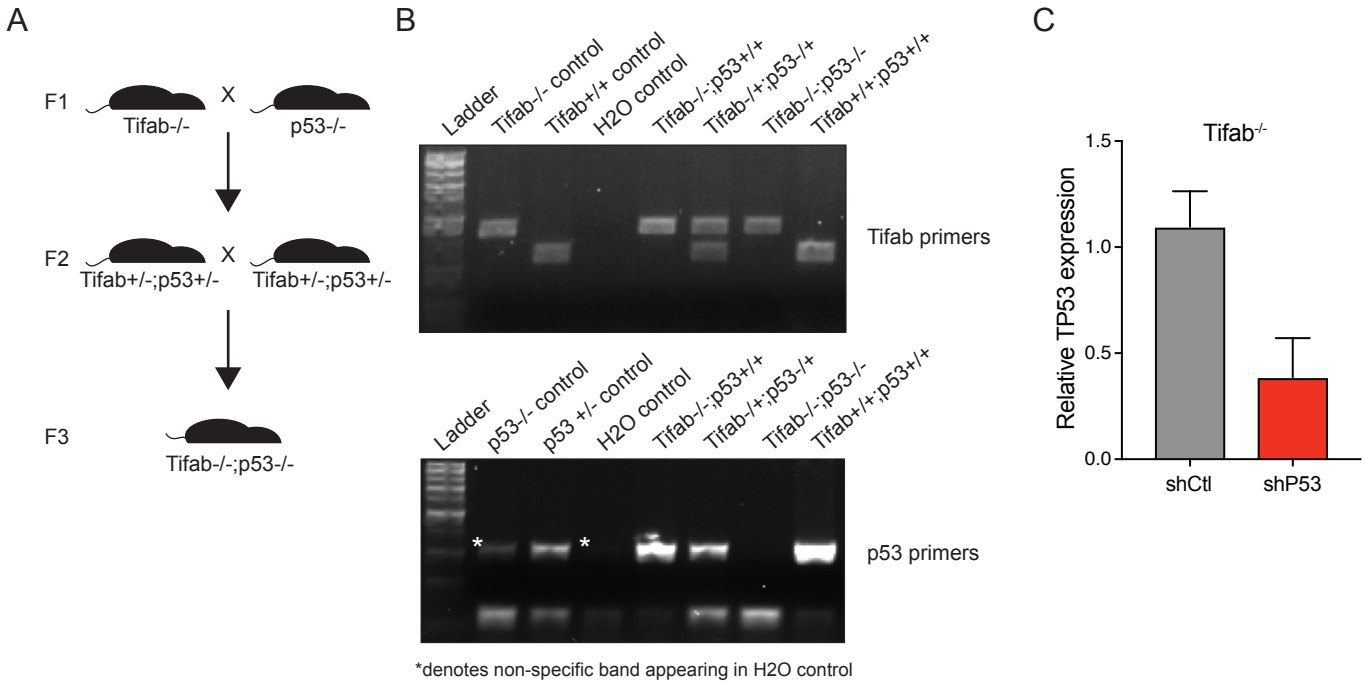

Figure S5. Generation of a Tifab$^{-/-}$;p53$^{-/-}$ double knockout mouse model (related to Figure 4). (A) Breeding strategy to generate Tifab$^{-/-}$;p53$^{-/-}$ mice. (**B**) Genotyping images for the Tifab locus (top gel) and the p53 locus (bottom gel) in the indicated mice, confirming deletion of Tifab and p53. **(C)** Relative TP53 mRNA expression in Tifab$^{-/-}$ BM LK cells transduced with lentiviral vectors encoding control shRNA (shCtl) or shRNAs targeting p53 (shP53).

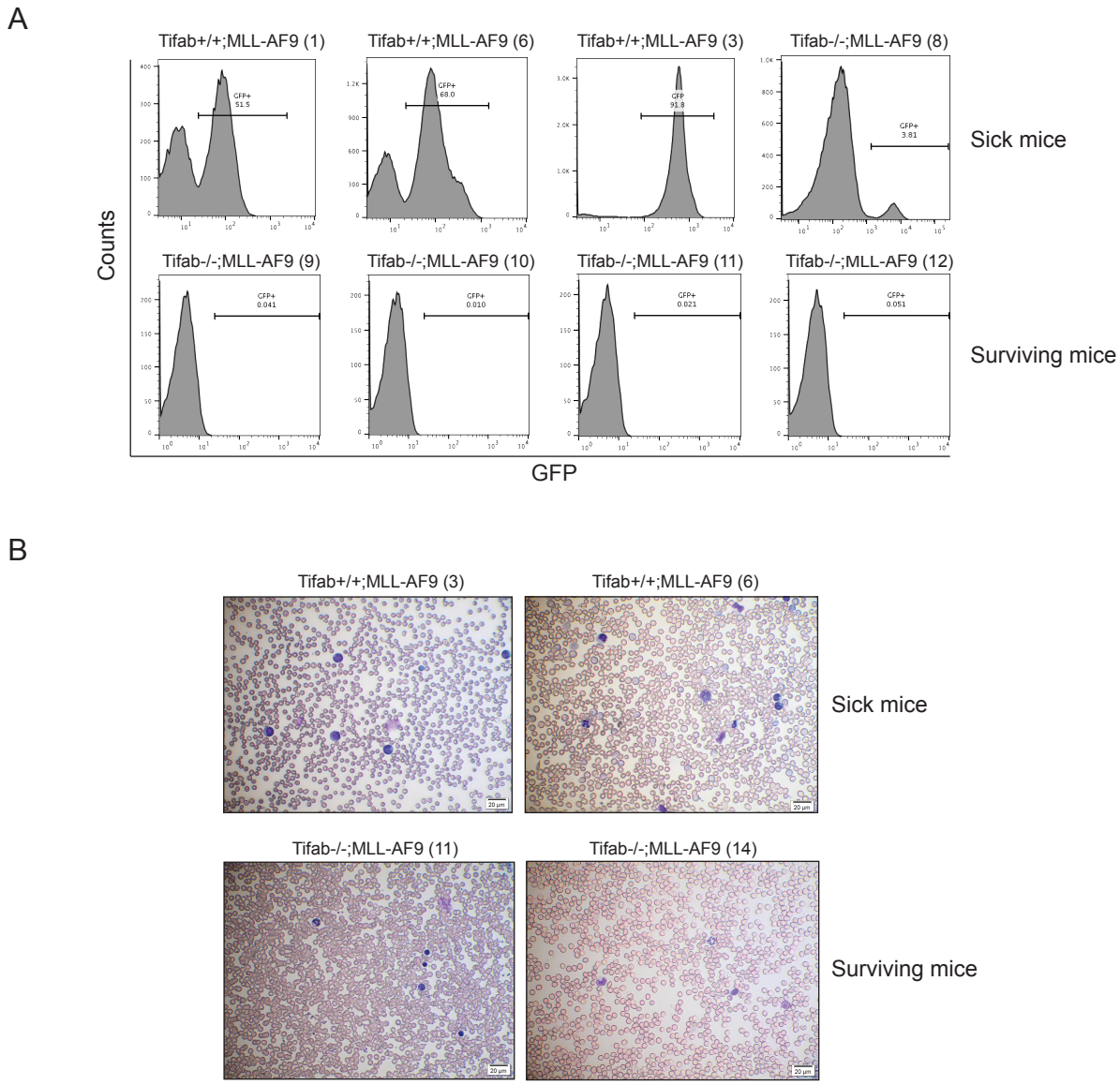

Figure S6. Peripheral blood analysis of Tifab+/+;MLL-AF9 and Tifab-/-;MLL-AF9 transplanted mice (related to Figure 6). (A) FACS histogram plots on PB mononuclear cells from sick (top row) and surviving (bottom row) mice that were transplanted with Tifab+/+;MLL-AF9 (GFP+) or Tifab-/-;MLL-AF9 (GFP+) cells. Bars indicate percent GFP+ cells in the PB. All mice transplanted with Tifab+/+;MLL-AF9 BM cells developed AML, while only one mouse transplanted with Tifab-/-;MLL-AF9 BM cells (mouse #8) developed AML. (**B**) Wright-Giemsa stained PB smears from two representative sick mice transplanted with Tifab+/+;MLL-AF9 BM cells (mouse #3 and #6) and two representative surviving mice transplanted with Tifab-/-;MLL-AF9 BM cells (mouse #11 and #14). The Tifab+/+;MLL-AF9 sick mice show evidence of myeloid blasts, indicated by larger, round white blood cells with a high nuclear to cytoplasmic ratio.

Table S1. TIFAB interactome analysis by mass spectrometry (related to Figure 1)

Rank	Protein	AVG Precursor Intensity	Rank	Protein	AVG Precursor Intensity	Rank	Protein	AVG Precursor Intensity	Rank	Protein	AVG Precursor Intensity
1	FABP5	7.25E+05	26	NEU2	2.01E+05	51	AHCYL1	9.86E+04	76	DDX17	6.34E+04
2	LDHA	4.38E+05	27	RAB7A	1.98E+05	52	ADSL	9.31E+04	77	SDHA	6.28E+04
3	RNH1	4.15E+05	28	**TIFA**	1.90E+05	53	SAMHD1	9.20E+04	78	ERO1L	6.25E+04
4	HSPB1	4.09E+05	29	GSTP1	1.89E+05	54	RPIA	8.31E+04	79	SERPINB1	6.13E+04
5	LMNA	3.48E+05	30	SSR4	1.88E+05	55	LRPPRC	8.31E+04	80	MPO	5.99E+04
6	ASPRV1	3.20E+05	31	DSC2	1.81E+05	56	GPS1	8.27E+04	81	PSMC1	5.98E+04
7	EEF1G	3.15E+05	32	COPS3	1.74E+05	57	ATP2A2	8.24E+04	82	PSMD2	5.70E+04
8	CALM1	3.01E+05	33	LGALS3	1.65E+05	58	AFG3L2	8.11E+04	83	ATP2A1	5.64E+04
9	CAPZA1	3.00E+05	34	PLEC	1.60E+05	59	PARK7	8.05E+04	84	GEMIN8	5.62E+04
10	TPM1	2.91E+05	35	**ANXA2**	1.58E+05	60	CANX	7.77E+04	85	CPD	5.61E+04
11	CALML3	2.86E+05	36	NCCRP1	1.54E+05	61	RCC2	7.64E+04	86	HSPH1	5.50E+04
12	SLC25A4	2.78E+05	37	PPL	1.49E+05	62	EIF4B	7.48E+04	87	TET2	5.12E+04
13	PRDX3	2.69E+05	38	RCL1	1.49E+05	63	DDX3X	7.45E+04	88	HADHA	5.10E+04
14	ANXA1	2.67E+05	39	PRDX6	1.41E+05	64	LBR	7.44E+04	89	LCP1	5.09E+04
15	TUFM	2.57E+05	40	EPPK1	1.30E+05	65	G6PD	7.27E+04	90	ATP1A1	4.96E+04
16	COPS4	2.53E+05	41	GDI2	1.28E+05	66	GSPT1	7.05E+04	91	HDAC2	4.90E+04
17	NME1	2.51E+05	42	AZGP1	1.24E+05	67	STT3A	6.99E+04	92	OGT	4.84E+04
18	SERPINB8	2.50E+05	43	ACTN1	1.21E+05	68	CCT6A	6.74E+04	93	C22orf28	4.60E+04
19	STRAP	2.41E+05	44	**USP15**	1.21E+05	69	CTPS1	6.72E+04	94	ATL3	4.60E+04
20	OLA1	2.23E+05	45	DBR1	1.13E+05	70	DOCK8	6.70E+04	95	FARSA	4.59E+04
21	TRIM29	2.15E+05	46	RAB2A	1.05E+05	71	CPT1A	6.60E+04	96	SRPR	4.54E+04
22	SLC25A5	2.14E+05	47	PKP3	1.03E+05	72	PRKDC	6.51E+04	97	UGGT1	4.54E+04
23	SERPINB5	2.08E+05	48	TMX3	1.03E+05	73	TRIM28	6.48E+04	98	BSG	4.53E+04
24	YOD1	2.03E+05	49	EVPL	1.02E+05	74	NSUN2	6.41E+04	99	HECTD3	4.53E+04
25	DDX21	2.02E+05	50	PRDX2	1.02E+05	75	TFRC	6.40E+04	100	AIFM1	4.37E+04